УДК 96.40.DE

Plyasheshnikov A., Lagutin A., Misaki A.,
Tiumentsev A.

Cherenkov Radiation of Electron-Photon Cascades in Water

A special highly effective scheme of the Monte Carlo method (the semyanalytical Monte Carlo method) is applied to the analysis of characteristics of the Cherenkov light produced in water by electron-photon cascades with energy $1 \div 10^5$ GeV. A detailed information about the depth-angular distribution of emitted Cherenkov photons useful for planning deep-underwater experiments on the registration of high energy muons and neutrinos is presented. The influence on the Cherenkov light characteristics of the light scattering is investigated. The region of validity of the model of a luminous point is analyzed.

Introduction

Last years a steady interest is observed in the scientific world to problems of astrophysics of high energy neutrino ($E_\nu \geq 100$ GeV). Due to the neutrality and high penetrating ability, high energy neutrinos can be useful for study of properties of interesting astrophysical objects (e.g. quazars, nuclei of seyfert galaxies, radiogalaxies etc. [1]). One of possible methods of registration of high energy neutrino is underwater detection. Experimental installations on deep-water detection (see, for example, russian project NT - 200 [2,3], at the depth at 1km in Like Baikal in Siberia; AMANDA [4], in deep polar ice at the South Pole; NESTOR [5], 3500m deep in the Mediterranean near Pylos, Greece) are usually spatial lattices of recording underwater elements (Cherenkov light detectors). Distance between recording elements should not be much more the length of transparency of water. The layer of water above installation provides protection from cosmic rays muons. Water between recording elements serves as a detector. Neutrinos interact with nuclei. Interactions give rise to secondary particles of cascade. Cherenkov radiation of cascade is registered by detectors.

Decoding signals of neutrino detectors one can determine the energy and direction of movement of the neutrino. A detailed theoretical information about multidimensional characteristics of Cherenkov radiation of electron-nuclear and electron-photon high energy cascades is necessary for optimization of algorithms of this decoding and determination of basic parameters of neutrino telescope (effective area of registration, angular and energy resolutions). The purpose of present works is an analisis of characteristics of the Cherenkov radiation in water from electron-photon cascades (EPC).

1. Simulation technique

The Monte Carlo method provides at present the most reliable way to calculate the multidimensional distributions of EPC parameters. The usage of exact data for the cross-sections of cascade particles, taking into account detectors properties and a possibility to consider inhomegeneous medium are well known advantages of this method.

The traditional (complete) Monte Carlo method has an essential drawback limiting essentially its applications. This drawback consists in a rapid (approximately linear) growth of the computational time with the energy of the particle initiating the cascade. That is why in the primary energy region $E \geq 10$ GeV the overwhelming majority of calculational results on the EPC Cherenkov light have been obtained by analylical and semyanalytical methods (see, for example, [6]).

In the present work a special scheme of the Monte-Carlo method (the semyanalytical Monte Carlo method, hereafter: SAMC) [7] is used to calculate the Cherenkov light characteristics of high energy EPC. Keeping all listed above advantages of the complete Monte Carlo the SAMC approach allows to weaken essentially dependence of the computational time on the primary energy (logarithmic growth). This circumstance gives us a possibility to analyze the Cherenkov light of EPC with energy up to 10^5 GeV.

The main idea of the SAMC is spliting the EPC into two parts: high energy ($E \geq E_{th}$; $E_{th} \simeq 1$ GeV in our case) and low energy ($E \leq E_{th}$) ones. The high energy part of the cascade is considered as a source of low energy γ-quanta and electrons. A special system of ajoint integro-differential cascade equations can be derived for the differential density of this source.

A number of assumptions can be made for inter-

actions of high energy cascade particles. Among them: the neglect of such processes as the energy losses for ionization, the compton scattering and the photoelectric absorption; the usage of simplified expressions for the bremstrahlung and pair production processes obtained in the full screening approximation; the usage of the small angle approximation for the multiple Coulomb scattering and the neglect of the displacement of particles with respect to the shower axis. These assumptions simplify essentially the shape of the cascade equations and allow to solve these equations by analytical and numerical (alternative to the Monte Carlo) methods.

Random values of initial phase coordinates are sampled in accordance with the mentioned above source density for a sufficiently great number of low energy cascade particles. The complete Monte Carlo method is applied to simulate subcascades created by such particles and to estimate characteristics of emitted by them Cherenkov light. The deposit to the Cherenkov light emission from the high energy part of the cascade is as a rule very small and can be neglected.

2. Depth-angular distribution of emitted Cherenkov photons

The size of the disk of EPC secondary particles (tens of centimeters) is incomparably smaller then distances between detectors of a neutrino telescope (tens of meters). In this connection, the characteristics of the Cherenkov radiation of EPC in water are often calculated with neglect of the size of the shower particle disk (see, for example, [6]). If, beside that, we neglect contribution to the light from scattered in water Cherenkov photons we come to a so called "model of a luminous point" (hereafter MLP). In the frame of this model all the Cherenkov light arriving to the detector at a fixed moment of time is emitted from a certain point located on the shower axis. In the approximation of MLP parameters of the EPC Cherenkov radiation can be expressed (see below) in terms of the depth-angular distribution of the number of emitted Cherenkov photons. That is why the basic features of this distribution are analyzed in the present section.

Definition of quantities

The *unnormalized depth-angular distribution of emitted photons* is a basic characteristics of the Cherenkov light discussed in this section. This quantity can be defined as the differential with respect to the depth, t, and the motion direction,

$\vec{\Omega}$, and averaged over random cascade realizations density of photons emitted by the EPC in the optical range of wavelengths $((0,325 \div 0,65)$ μm in our case). Let us denote this quantity as $n(E,t,\vartheta)$ where $cos\vartheta = \vec{\Omega} \cdot \vec{\Omega}^*$ ($\vec{\Omega}^*$ is the shower axis direction).

Integration of differential density $n(E,t,\vartheta)$ over the motion direction of emitted photons leads to *the unnormalized depth distribution* of the number of emitted photons:

$$n(E,t) = 2\pi \int\limits_0^\pi n(E,t,\vartheta) \sin\vartheta d\vartheta. \qquad (1)$$

Additional integration over the depth results in *the total number* of emitted photons:

$$n(E) = \int\limits_0^\infty n(E,t)dt =$$
$$= 2\pi \int\limits_0^\infty dt \int\limits_0^\pi n(E,t,\vartheta) \sin\vartheta d\vartheta. \quad (2)$$

Integration of $n(E,t,\vartheta)$ over the depth results in *the unnormalized equilibrated angular distribution* of emitted photons:

$$n(E,\vartheta) = \int\limits_0^\infty n(E,t,\vartheta)dt \qquad (3)$$

(i.e. the distribution averaged over the depth of the cascade development).

Two kinds of normalized angular distribution will be discussed below. They are *the equilibrated angular distribution*:

$$f(E,\vartheta) = \frac{n(E,\vartheta)}{n(E)}. \qquad (4)$$

and *the unequilibrated angular distribution*:

$$f(E,t,\vartheta) = \frac{n(E,t,\vartheta)}{n(E,t)}. \qquad (5)$$

Quantities $f(E,\vartheta)$ and $f(E,t,\vartheta)$ satisfy to obvious normalization conditions

$$2\pi \int\limits_0^\infty f(E,\vartheta) \sin\vartheta d\vartheta =$$
$$= 2\pi \int\limits_0^\pi f(E,t,\vartheta) sin\vartheta d\vartheta = 1. \quad (6)$$
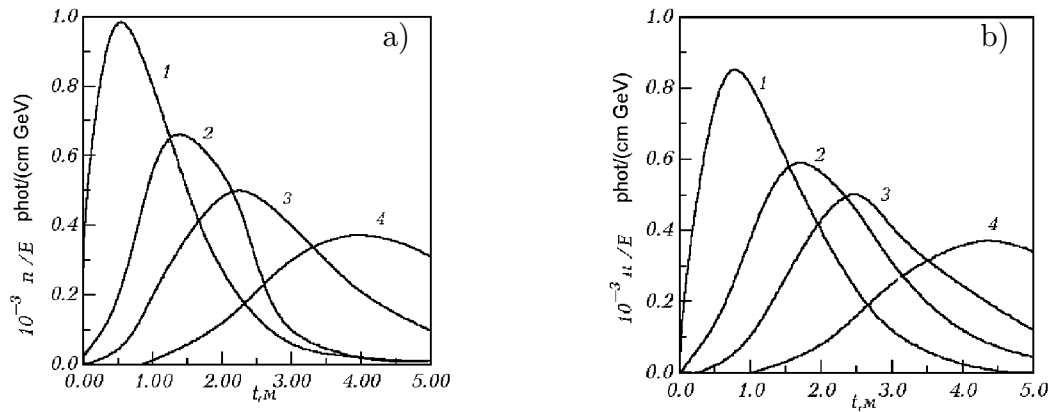
Figure 1. The unnormalized depth distributions of the number of emitted Cherenkov photons for cascades induced by the electron (a) and the photon (b). $E = 1$GeV (1), $E = 10$GeV (2), $E = 10^2$GeV (3), $E = 10^4$GeV (4)

Total number of photons

Our calculations showed that in the energy range $(1 - 10^5)$ GeV dependence $n(E)$ can be approximated by the following function:

$$n(E) = 1.45 \cdot 10^5 E, \qquad (7)$$

where E is measured in GeV. This relation is valid for the EPC created by both primary particles.

Table 1

The average number of Cherenkov photons emitted in the optical range of wavelengths by a single electron per a unit length of its way in water

E, MeV	0.77	1.00	1.50	2.50	5.50	∞
$n_0(E)$, phot/cm	0.0	170	255	289	303	306

Depth distribution

Examples of unnormalized depth distributions of emitted Cherenkov photons are presented in fig.1. As it is seen from the figure, dependence of $n(E,t)$ on the depth, t, of the shower development has a local maximum. The position of this maximum, t_m, moves slowly towards larger values of t with the primary energy growth. The value of t_m for the primary photon is somewhat greater ($\sim$ 0.25-0.30 m) in comparison to the electron initiated shower.

In the case of $t \to 0$ the main contribution to the value of $n(E,t)$ is provided by the Cherenkov radiation of the primary particle. That is why for the photon induced shower

$$\lim_{t \to 0} n(E,t) = 0 \qquad (8)$$

For the shower from primary electron

$$\lim_{t \to 0} n(E,t) = n_0(E) \qquad (9)$$

where $n_0(E)$ is the average number of Cherenkov photons emitted by the electron of energy E per a unit length of its way in water.

One can see from tab.1 that $n_0(E)$ is different from zero for energy values $E > 0,77$ MeV, grows monotonously with E and comes assimptotically to its limiting value $\simeq 300$ phot/cm. Therefore, $n(E, t = 0) \simeq 300$ phot/cm for all curves of fig.1 corresponding to the electron initiated EPC.

In tab.2 we present the ratio $n(E,t)/N_e(E,t)$ in which $N_e(E,t)$ defines the average total number of cascade charged particles (electrons and positrons) at the depth t of the cascade development. One can see that the noted above ratio depends very weakly on the primary energy and the depth . Therefore, the following relation takes place:

$$n(E,t) \simeq 300 \cdot N_e(E,t). \qquad (10)$$

Equilibrated angular distribution

Our analysis showed that in the primary energy region $E \geq 1$ GeV the shape of the normalized

Table 2

The ratio $n(E,t)/N_e(E,t)$ for the primary photon

$E,$	$t_/t_m$								
GeV	0.05	0.10	0.20	0.40	0.70	1.00	1.50	2.00	3.00
1	303	303	302	301	300	299	298	296	296
10	304	303	301	300	299	298	297	295	—

Table 3

The equilibrated angular distribution of emitted photons

$\cos\vartheta$	$f(\vartheta)$	$\cos\vartheta$	$f(\vartheta)$	$\cos\vartheta$	$f(\vartheta)$	$\cos\vartheta$	$f(\vartheta)$
0.987	0.079	0.769	0.721	0.644	0.185	0.075	0.0209
0.938	0.105	0.756	1.393	0.606	0.139	−0.05	0.0162
0.887	0.150	0.744	1.038	0.537	0.0913	−0.25	0.0113
0.837	0.236	0.731	0.647	0.488	0.0706	−0.45	0.0079
0.813	0.318	0.719	0.480	0.412	0.0525	−0.65	0.0055
0.794	0.414	0.694	0.319	0.325	0.0392	−0.85	0.0036
0.781	0.523	0.669	0.236	0.225	0.0209	−0.95	0.0027

equilibrated angular distribution $f(E,\vartheta)$ does not depend practically on the energy and type of the primary particle, i.e. $f(E,\vartheta) \simeq f(\vartheta)$. The data on distribution $f(\vartheta)$ are showed in tab. 3. The following conclusions can be made from the table.

- Function $f(\vartheta)$ has a sharp local maximum near $\vartheta = \arccos(1/m)$ (m = 1,33 is the refraction parameter of water). This maximum is caused by contribution from high energy electrons moving along the shower axis. These electrons emit the Cherenkov light along a conic surface having the opening angle $\vartheta_0(E) \simeq \vartheta_0(E = \infty) = \arccos(1/m)$.

- Function $f(\vartheta)$ has a long flat tail in the region of large values of ϑ. The main contribution to this tail is given by cascade electrons having large values of the multiple scattering angle.

Figure 2. The normalized angular distribution of emitted photons for the electron induced EPC. $E = 10^3$ GeV. $u = 0.3$ (1), $u = 1$ (2), $u = 3$ (3)

Unequilibrated angular distribution

Our analysis showed that dependence of the normalized angular distribution $f(E,t,\vartheta)$ on the EPC primary energy can be essentially weaken , if one uses instead of depth t a new variable $u = t/t_m$ where t_m is the depth of the maximum of the cascade electron number (the data on t_m are presented in tab. 4).

Moreover, for each value of variable u defining a degree of the shower development a certain ul-
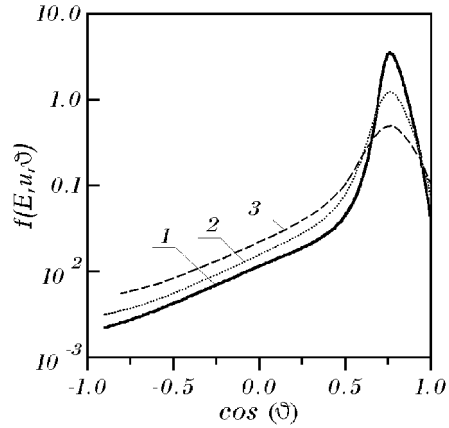
Table 4

Data on the position of the maximum number of cascade electrons $t_m(m)$ for primary electron (1) and primary photon (2)

E, GeV	1	3	10	30	10^2	10^3	10^4	10^5
1	0.64	1.02	1.44	1.85	2.29	3.13	3.95	4.76
2	0.90	1.29	1.74	2.12	2.57	3.42	4.24	5.07

Table 5

Data on the ultimate value E_∞ (GeV) of the primary energy above which the normalized angular distribution $f(E, u, \vartheta)$ does not depend on E (line 1 – primary electron, line 2 – primary photon) or on the nature of the primary particle (line 3)

	u			
	0.3	0.5	1.0	2.0
1	10^4	10^2	10	1
2	10^3	10^2	3	1
3	10^2	10	3	1

timate value of primary energy, E_∞, exists above which the normalized angular distribution does not depend on the primary energy E. The data on E_∞ are given in tab. 5. One can see from this table that E_∞ decreases with a growth of u and varies from $E_\infty \sim 10^3 \div 10^4$ GeV ($u = 0,3$) down to $E_\infty \sim 1$ GeV ($u = 2$). Under the same other conditions smaller values of E_∞ correspond to the primary photon. Beside that, there exists some ultimate value of the primary energy, E_∞, such as the shape of distribution $f(E, u, \vartheta)$ does not depend on the type of the primary particle in the energy region $E > E_\infty$. This quantity also decreases with u and varies from $\sim 10^2$ GeV down to ~ 1 GeV.

In tab.6 we present data concerning the normalized angular distribution $f(E, u, \vartheta)$ for the following ranges of independent variables : $1 \le E \le 10^5$GeV, $0, 3 \le u \le 3$, $0 \le \vartheta \le \pi$. The data of the table correspond to the EPC from primary photon. The data of tab.6 (together with tab.7) give also a possibility to calculate function $f(E, u, \vartheta)$ for the EPC induced by primary electron. Some examples of unequilibrated angular distributions $f(E, u, \vartheta)$ are also presented in fig.2. One can see from the figure that dependence of the angular distribution on angle ϑ has a local maximum. The position of this maximum depends weakly on E and u and is close to $\vartheta_m = \arccos(1/m) \simeq 40^o$.

For a fixed value of E the width of distribu-

tion $f(E, u, \vartheta)$ increases with a growth of u. This circumstance can be explained by an increase of the multiple scattering of cascade electrons with u. Comparing data of tab. 3 and tab.6 one can establish that in the vicinity to the shower maximum ($u \approx 1$) the unequilibrated angular distribution $f(E, u, \vartheta)$ has a shape similar to the shape of the equilibrated distribution $f(\vartheta)$. For a fixed value of u $f(E, u, \vartheta)$ becomes widther with a growth of E.

3. Influence of light scattering and validity of MLP

As it was noted above the mean values of characteristics of the EPC Cherenkov light can be expressed in terms of the depth-angular distribution of emitted photons, if one neglects the size of the shower particle disk and the contribution from the scattered light. A model of a luminous point (MLP) corresponds to this approach. An obvious advantage of this model is a possibility of an essential reduction of amount of calculational data needed for planning and data analysis of deep-underwater experiments.

In this section we analyze data obtained with taking into account the size of the shower particle disk and the Cherenkov light scattering. Such an approach enables to establish the region of the MLP validity.

Calculation details.

The complete Monte Carlo method is applied to simulate the transport of Cherenkov photons in water. The absorption and scattering processes are taken into account. It is supposed that the total cross-sections of these processes do not depend on the photon wavelength and both are equal to 1/15 m^{-1}. The scatering indicatrissa is also considered to be independent on the wavelength. The experimental data of the NT-200 collaboration [8] are used to describe this quantity (see tab. 8).

All results presented below correspond to the

Table 6

The normalized angular distribution of emitted Cherenkov photons for the photon induced EPC

u	0.3				0.5			
E, GeV	1	10	10^3	10^5	1	10	10^3	10^5
$\cos\vartheta$								
0.987	0.0436	0.0583	0.0434	0.0442	0.0519	0.0628	0.0600	0.0573
0.938	0.0550	0.0710	0.0589	0.0593	0.0725	0.0812	0.0808	0.0846
0.887	0.0763	0.109	0.0906	0.0899	0.0988	0.123	0.117	0.119
0.837	0.116	0.140	0.149	0.161	0.167	0.202	0.197	0.202
0.813	0.190	0.218	0.211	0.237	0.259	0.279	0.276	0.275
0.794	0.313	0.298	0.310	0.339	0.385	0.385	0.350	0.374
0.781	0.499	0.474	0.460	0.482	0.577	0.535	0.499	0.501
0.769	1.01	0.723	0.757	0.755	0.936	0.843	0.830	0.799
0.756	3.22	3.49	3.74	3.61	2.23	2.17	2.40	2.42
0.744	2.31	1.72	1.57	1.48	1.74	1.49	1.43	1.35
0.731	0.854	0.631	0.692	0.629	0.862	0.713	0.710	0.671
0.719	0.375	0.391	0.421	0.421	0.508	0.483	0.447	0.442
0.694	0.218	0.235	0.220	0.237	0.285	0.269	0.269	0.273
0.669	0.147	0.140	0.170	0.151	0.182	0.202	0.206	0.203
0.644	0.103	0.109	0.122	0.123	0.132	0.150	0.148	0.155
0.606	0.0667	0.0873	0.0967	0.945	0.0877	0.108	0.109	0.112
0.537	0.0437	0.0534	0.0585	0.0555	0.0622	0.0747	0.0663	0.0725
0.488	0.0445	0.0362	0.0405	0.0422	0.0470	0.0571	0.0522	0.0542
0.412	0.0281	0.0348	0.0267	0.0300	0.0319	0.0421	0.0380	0.0404
0.325	0.0194	0.0297	0.0238	0.0233	0.0284	0.0304	0.0305	0.0305
0.225	0.0180	0.0185	0.0178	0.0194	0.0193	0.0225	0.0232	0.0230
0.075	0.0148	0.0120	0.0125	0.0132	0.0151	0.0139	0.0155	0.0168
-0.05	0.0119	0.0101	0.0107	0.0105	0.0113	0.0126	0.0131	0.0133
-0.25	0.0076	0.0073	0.0079	0.0076	0.0080	0.0086	0.0088	0.0089
-0.45	0.0047	0.0041	0.0044	0.0052	0.0064	0.0060	0.0061	0.0065
-0.65	0.0037	0.0027	0.0037	0.0040	0.0039	0.0041	0.0042	0.0043
-0.85	0.0023	0.0028	0.0022	0.0025	0.0026	0.0029	0.0029	0.0030

Table 6

(continuation)

u	0.8			1.2		1.7	2.3	3.0
E, GeV	1	10	10^5	1	10^5	10^5	10^5	10^5
$\cos\vartheta$								
0.987	0.632	0.0675	0.0716	0.0841	0.0849	0.0915	0.107	0.121
0.938	0.0874	0.0954	0.0961	0.108	0.0108	0.121	0.130	0.169
0.887	0.131	0.136	0.140	0.154	0.154	0.173	0.173	0.211
0.837	0.219	0.222	0.227	0.250	0.245	0.259	0.281	0.328
0.813	0.304	0.305	0.311	0.346	0.337	0.331	0.340	0.311
0.794	0.419	0.423	0.420	0.433	0.431	0.421	0.395	0.341
0.781	0.591	0.549	0.525	0.557	0.517	0.501	0.496	0.453
0.769	0.864	0.792	0.771	0.746	0.695	0.648	0.538	0.486
0.756	1.52	1.56	1.61	1.04	1.18	0.934	0.674	0.495
0.744	1.24	1.23	1.16	0.967	0.938	0.817	0.619	0.847
0.731	0.775	0.689	0.673	0.671	0.630	0.583	0.541	0.451
0.719	0.558	0.482	0.480	0.505	0.488	0.479	0.457	0.132
0.694	0.329	0.317	0.311	0.342	0.336	0.329	0.353	0.355
0.669	0.231	0.230	0.221	0.255	0.245	0.253	0.268	0.260
0.644	0.161	0.169	0.182	0.204	0.195	0.199	0.215	0.228
0.606	0.124	0.137	0.135	0.138	0.139	0.154	0.173	0.154
0.537	0.0821	0.0858	0.0825	0.0978	0.0952	0.0995	0.108	0.145
0.488	0.0629	0.0637	0.0637	0.0697	0.0722	0.0817	0.0919	0.0810
0.412	0.0436	0.0477	0.0496	0.0518	0.0548	0.0585	0.0666	0.0675
0.325	0.0315	0.0333	0.0356	0.0398	0.0418	0.0452	0.0511	0.0570
0.225	0.0256	0.0258	0.0270	0.0303	0.0314	0.0349	0.0388	0.0362
0.075	0.0177	0.0180	0.0193	0.0199	0.0221	0.0248	0.0264	0.0265
-0.05	0.0131	0.0145	0.0152	0.0161	0.0171	0.0179	0.0222	0.189
-0.25	0.0102	0.0102	0.0106	0.0117	0.0116	0.0127	0.0133	0.133
-0.45	0.0067	0.0071	0.0076	0.0076	0.0086	0.0089	0.0110	0.0085
-0.65	0.0040	0.0049	0.0050	0.0055	0.0057	0.0062	0.0069	0.0053
-0.85	0.0034	0.0028	0.0032	0.0034	0.0034	0.0042	0.0047	0.0051

Table 7

The ratio of normalized angular distributions corresponding to different primary particles (γ/e)

		$\cos\vartheta$						
u	E, GeV	0.912	0.769	0.756	0.744	0.731	0.512	0.225
0.3	1	1.30	1.38	0.78	0.72	1.62	0.88	1.17
	10	1.26	0.95	0.88	0.91	0.93	1.33	1.11
	10^2	1.03	1.03	0.99	0.96	1.02	0.98	1.11
	10^3	1.00	0.97	1.01	1.03	1.07	0.96	1.03
0.5	1	1.21	0.89	0.82	0.75	1.08	1.25	1.22
	3	0.94	1.00	1.01	0.91	1.04	1.07	1.07
	10	1.21	1.01	0.86	0.89	1.02	1.13	1.24
	10^2	1.08	1.01	0.99	1.00	1.00	0.97	1.11
1.0	1	1.17	0.82	0.96	0.88	0.89	1.18	1.04
	3	1.00	0.97	1.00	0.97	0.97	1.05	1.06
	10	1.00	1.01	1.00	1.01	1.00	0.97	1.02
2.0	1	1.12	0.90	0.95	0.95	0.91	1.05	1.11
	3	1.01	1.00	1.07	1.05	0.99	1.00	1.10
	10	1.00	0.97	1.06	1.01	0.99	0.99	1.01

Table 8

Dependence of the scattering indicatrissa $\chi(\cos\vartheta)$ on the cosine of the scattering angle. $\int_{-1}^{+1}\chi(\cos\vartheta)d\cos\vartheta = 2$

$\cos\vartheta$	$\chi(\cos\vartheta)$	$\cos\vartheta$	$\chi(\cos\vartheta)$	$\cos\vartheta$	$\chi(\cos\vartheta)$
1.000	4690	0.766	0.53	−0.500	0.065
0.999	200	0.642	0.32	−0.642	0.063
0.996	63.2	0.500	0.20	−0.766	0.063
0.991	23.8	0.342	0.15	−0.866	0.062
0.984	11.2	0.174	0.110	−0.940	0.062
0.966	5.02	0.000	0.089	−0.985	0.062
0.940	2.52	−0.174	0.080	−1.00	0.061
0.866	1.06	−0.342	0.073		

Table 9

Values of function $C(\theta)$

$\cos\theta$	$C(\theta)$	$\cos\theta$	$C(\theta)$	$\cos\theta$	$C(\theta)$
1.00	4.64	0.30	3.10	-0.60	0.76
0.93	4.66	0.20	2.86	-0.70	0.27
0.88	4.64	0.10	2.60	-0.78	0.20
0.81	4.56	0.00	2.34	-0.80	0.13
0.76	4.47	-0.10	2.10	-0.85	0.09
0.70	4.29	-0.20	1.84	-0.90	0.02
0.50	3.66	-0.40	1.32		
0.40	3.38	-0.50	1.04		

Cherenkov light detector "Quazar" [8].The effective area of registration, S, is a basic characteristics of this detector. It can be defined by the following expression:

$$S = C(\theta)R^2, \tag{11}$$

where $R = 17.5$, θ is the angle between the optical axis of the detector $(\vec{\Omega}_0)$ and the arrival direction of registered photons $(\vec{\Omega})$. The values of function C are presented in tab. 9.

Two different directions of the optical axis of "Quazar", $\vec{\Omega}_o$, are considered in our analysis: parallel and antiparallel to the shower axis direction $\vec{\Omega}^*$.

The following characteristics of the EPC Cherenkov light are considered in this section.

- The averaged over cascade realizations unnormalized temporal distribution of the number of registered photons, $I(z,r,\tau)$, where z is the depth, r is the distance from the shower axis. The zero value of τ corresponds to the moment of appearance of initiating cascade particle.

- The mean number of photons registered by the detector

$$\bar{q}(z,r) = \int\limits_{0}^{\infty} I(z,r,\tau)d\tau. \tag{12}$$

54

- The normalized temporal distribution of the number of registered photons

$$f(z, r, \tau) = I(z, r, \tau)/\bar{q}(z, r). \qquad (13)$$

Expressions concerning MLP

As it was noted above in the frame of the MLP characteristics of the EPC Cherenkov radiation can be expressed in terms of the depth-angular distribution of number of emitted photons. For the quantities analyzed in this section this can be achieved with the help of the following formulae:

$$\bar{q}(z, r) = \int\limits_0^\infty n(E, \tilde{z}, \cos\vartheta) d^{-2} e^{-\sigma d} S(\vec{\Omega}\vec{\Omega}_0) d\tilde{z}, \qquad (14)$$

$$I(z, r, \tau) = n(E, \tilde{z}, \cos\vartheta) d^{-2} e^{-\sigma d} S(\vec{\Omega}\vec{\Omega}_0) |\frac{d\tilde{z}}{d\tau}|. \qquad (15)$$

In (14), (15) the quantities have the following meaning:

$$\frac{d\tilde{z}}{d\tau} = c \cdot [1 + \frac{m(\tilde{z} - z)}{d}]^{-1}; \qquad (16)$$

$$d = [(\tilde{z} - z)^2 + r^2]^{1/2}, \quad \cos\vartheta = \frac{z - \tilde{z}}{d}; \qquad (17)$$

$n(E, z, \vartheta)$ is defined above unnormalized depth-angular distribution of emitted photons; m is the refraction parameter of water; c is the speed of light in the vacuum; σ is the total cross-section of photon interactions; S is determined by (11); the sense of vector $\vec{\Omega}$ is clear from fig.3.

It should be noted also that variables τ and $\tilde{z}$ are connected by the following relation:

$$\tau = (\tilde{z} + [(z - \tilde{z})^2 + r^2]^{1/2})/c. \qquad (18)$$

Results

In fig.4 we present data on the normalized temporal distribution of registered Cherenkov photons, $f(z, r, \tau)$, calculated under different assumptions: exact data; data without taking into account the contribution from the scattered light; data obtained in the frame of the MLP (i.e., with usage of formulae (14), (15)). As it is seen from the
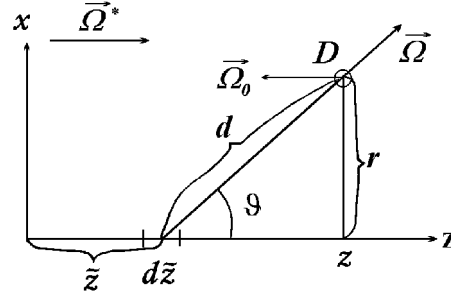

Figure 3. To evaluation of MLP expressions

figure there exists a significant difference between the exact and MLP data. At the same time, the data without the contribution of scattered photons are in a resonable agreeement with the MLP data. Therefore, the neglect of the light scattering is an essentially more serious approximation in comparison to neglecting a finite size of the shower particle disk.

In fig.5 the comparison of exact results and the MLP data is presented. The data of this figure correspond to higher values of the primary energy ($E_\gamma = 10^3$ GeV) and illustrate dependence of the data discrepancy on the detector position (it is defined by the depth z and the lateral displacement r). The following conclusions can be made from the figure.

- The MLP gives an overestimated value of the magnitude of the normalized temporal distribution. The discrepancy in the magnitude increases with the depth growth and can reach up to a factor of $(3 \div 4)$.

- The MLP gives an underestimated value for the width of the temporal distribution. The difference in the width can reach as much as $(2 \div 3)$ times.

- The exect temporal distribution has a long flat tail which is caused by the Cherenkov photon scattering. The contribution of the tail to the total number of registerd photons increases with the growth of lateral displacement r of the detector.

- The arrival time of the first Cherenkov photon (on the figure it corresponds to the pulse beginning) is correctly reproduced by the MLP. Difference in the position of the forward point of the pulse does not exceed as a rule the size of the histogramm bin (2 ns).

In the model of a luminous point all photons emitted at a certain depth $\tilde{z}$ of the shower development give a contribution to a strictly certain point
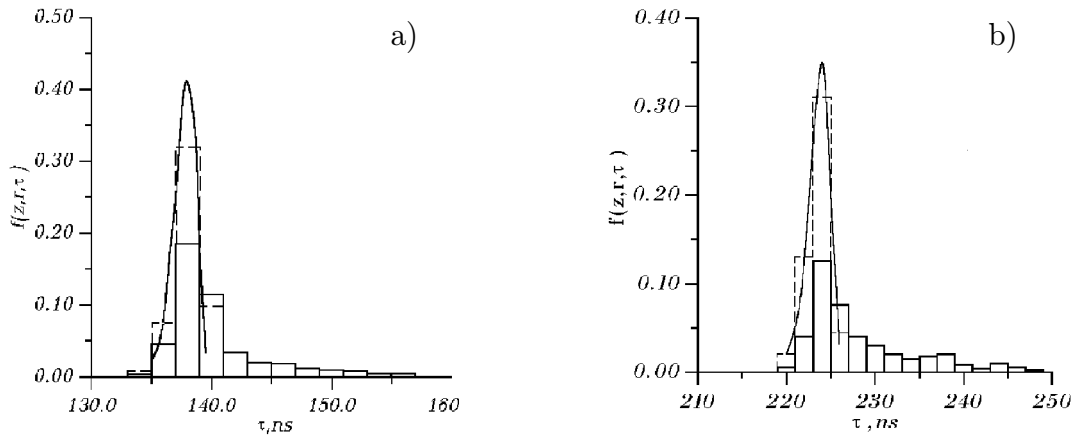
Figure 4. The normalized temporal distributions of the number of registered Cherenkov photons. $E_\gamma = 10$ GeV. Solid histogramms — exact calculation, dashed histogramms — calculation without the light scattering, curves — MLP. $z = 30$ m (a), 50 m (b); $r = 10$ m
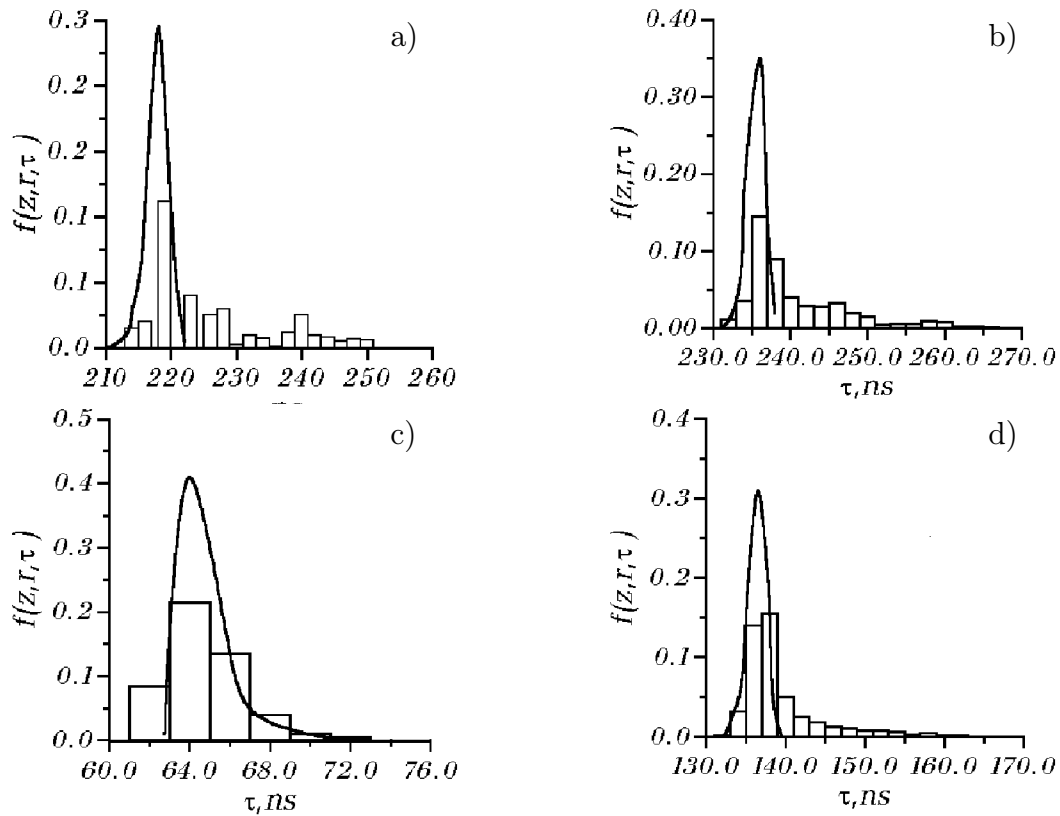

Figure 5. The normalized temporal distributions of the number of registered photons. $E_\gamma = 10^3$ GeV, $\vec{\Omega}_0 \vec{\Omega}^* = -1$. Histogrammes — exact calculation, curves — MLP . $z = 50$ m (a,b), 10 m (c), 30 m (d); $r = 5$ m (a), 20 m (b), 10 m (c,d)

Table 10
The ratio of mean numbers of Cherenkov photons registered by "Quazar" within the time interval $\Delta\tau$ and corresponding to the exact (nomenator) and MLP (denominator) data. $E_\gamma = 10^3$ GeV, $\vec{\Omega}_0\vec{\Omega}^* = -1$

r, m	0	10	20	30	40	50
$\Delta\tau = 10$ ns, $z = 30$ m	0.84	0.77	0.77	0.76	0.72	0.64
$\Delta\tau = 20$ ns, $z = 50$ m	0.96	1.00	0.87	0.89	0.91	0.92
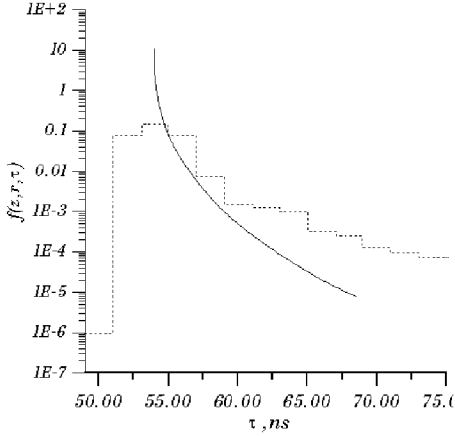
Figure 6. The normalized temporal distributions according to exact data (hist.) and MLP (curve). $E_\gamma = 10^3$ GeV, $\vec{\Omega}_0\vec{\Omega}^* = -1$. $z = 10$ m, $r = 7$ m

Table 11
The ratio of the numbers of Cherenkov photons registerd by "Quazar" and corresponding to the exact (nominator) and MLP (denominator) data. $E_\gamma = 10^3$ GeV

		r, m				
$\vec{\Omega}_0\vec{\Omega}^*$	z, m	0.5	5	10	20	50
-1	-30	3070	59.3	59.5	10.3	2.06
	0	3.52	1.16	1.12	1.15	1.13
	30	1.10	1.26	1.17	0.798	1.20
	70	0.463	1.23	1.29	1.01	0.589
$+1$	-30	1.48	1.81	1.83	1.64	1.30
	0	1.19	1.24	1.27	1.33	1.36
	30	4913	54.5	13.6	1.41	1.71
	70	0.463	1.22	1.25	1.01	0.589

τ of the temporal distribution. Relation between values $\tilde{z}$ and τ is determined by formula (18). Differentiating (18) one can check that at

$$\tilde{z}_0 = z - r(m^2 - 1)^{-1/2} \qquad (19)$$

derivative $d\tau/d\tilde{z}$ is equal to zero. That is why the reverse derivative $d\tilde{z}/d\tau$ becomes infinite at this point. Therefore, the temporal distribution calculated in the MLP approximation has an integrated peculiarity at the point

$$\tau_0 = \left(z + r[m^2 - 1]^{-1/2} \right)/c, \qquad (20)$$

corresponding to the pulse beginning. This peculiarity can influence considerably the shape of the temporal distribution, if an essential amount of Cherenkov photons is emitted near $\tilde{z}_o$.

The latter takes place, if $\tilde{z}_o \simeq z_m$ where z_m is the shower maximum position. This case is presented in fig.6. As it is seen from the figure the infiniteness of $d\tilde{z}/d\tau$ influences cathastphicaly the shape of the temporal distribution. The difference between exact and MPL data can reach a factor of $10 \div 100$.

To suppress the background light connected with the luminosity of water it is planned in the experiment NT-200 to restrict the time of the light registration measuring it from the moment of arriving to the detector the first Cherenkov photon. In this connection we show in tab. 10 the ratio of average responses of detector "Quazar" coresponding to two different ways of calculation (exact and MLP data) and two typical values of the time restriction interval (10 and 20 ns). It is seen from the figure that the usage of the MLP can lead to an essential overestimation of the detector responce.

In tab.11 we present the ratio of total number of regisrered photons corresponding to exact calculation and MLP. No conditions restricting the arrival time are used in this table. The following conclusions can be reached from the table.

- In general, the MLP satisfactorily describes mean value of the detector response.

- There exists some region of observation point locations in which the MLP gives an underestimated value of the detector responce. This is a region where unscattered photons arrive to the detector having motion directions $\vec{\Omega}$ antiparallel to the direction $\vec{\Omega}_o$ of the detector optical axis. Difference between the exact and MLP data can reach here up to as much as hundreds times.

The latter conclusion can be explained by the following way. The effective area of detector falls very rapidly (see tab.9), if $\vec{\Omega}\vec{\Omega}_0 \to -1$. Therefore, in this region the contribution is important from scattered photons which come to the detector from arbitrary directions and which are not taken into account in the MLP. The contribution of such photons can be important in the analysis of the flux of neutrinos coming from the opposite side of the Earth. The usage of the MLP leads in this situation to an essential underestimation of the contribution from atmospheric muons.

References

1. Berezinsky V. S., Bulanov S. V., et.al. Astrophysics of Cosmic Rays. M.: Nauka, 1984, 360 p.

2. Belolaptikov I. A. et.al. // Proc. of the 24-th Int. Cosmic Ray Conf., Rome, 1995, v.1, p.742.

3. Belolaptikov I. A. et.al. // Astroparticle Physics, v.47, 1997, p.251.

4. P. C. Mock et.al. // Proc. of the 24-th Cosmic Ray Conf., Rome, 1995, v.1, p.758.

5. S. Bottai et.al. // Proc. of the 24-th Int. Cosmic Ray Conf., Rome, 1995, v.1, p.1080.

6. Beliaev A. A., Ivanenko I. P., et.al. Electron-Photon Cascades in Cosmic Rays at Superhigh Energies. M.: Nauka, 1980, 306p.

7. Konopelko A., Plyasheshnikov A. // Nuclear Physics B. (Proc. Suppl.), v.52B, p.152.

8. Bugaev E. V., et.al. INR Preprint P-0508, Moscow, 1987.